

OUTGASSING BEHAVIOR OF C/2012 S1 (ISON) FROM 2011 SEPTEMBER TO 2013 JUNE

KAREN J. MEECH^{1,2}, BIN YANG^{1,2}, JAN KLEYNA^{1,2}, MEGAN ANSDELL², HSIN-FANG CHIANG^{1,2}, OLIVIER HAINAUT³,
JEAN-BAPTISTE VINCENT⁴, HERMANN BOEHNHARDT⁴, ALAN FITZSIMMONS⁵, TRAVIS RECTOR⁶, TIMM RIESEN^{1,2},
JACQUELINE V. KEANE^{1,2}, BO REIPURTH^{1,2}, HENRY H. HSIEH^{2,A}, PETER MICHAUD⁷, GIANNANTONIO MILANI^{8,B}, ERIK
BRYSSINCK^{9,B}, ROLANDO LIGUSTRI^{10,B}, ROBERTO TRABATTI^{11,B}, GIAN-PAOLO TOZZI¹², STEFANO MOTTOLA¹³, EKKEHARD
KUEHRT¹³, BHUWAN BHATT¹⁴, DEVENDRA SAHU¹⁴, CAREY LISSE¹⁵, LARRY DENNEAU², ROBERT JEDICKE², EUGENE
MAGNIER², RICHARD WAINSCOT².

Submitted, 2013-08-25; Revised, 2013-09-07; Accepted, 2013-09-09

ABSTRACT

We report photometric observations for comet C/2012 S1 (ISON) obtained during the time period immediately after discovery ($r=6.28$ AU) until it moved into solar conjunction in mid-2013 June using the UH2.2m, and Gemini North 8-m telescopes on Mauna Kea, the Lowell 1.8m in Flagstaff, the Calar Alto 1.2m telescope in Spain, the VYSOS-5 telescopes on Mauna Loa Hawaii and data from the CARA network. Additional pre-discovery data from the Pan STARRS1 survey extends the light curve back to 2011 September 30 ($r=9.4$ AU). The images showed a similar tail morphology due to small micron sized particles throughout 2013. Observations at sub-mm wavelengths using the JCMT on 15 nights between 2013 March 9 ($r=4.52$ AU) and June 16 ($r=3.35$ AU) were used to search for CO and HCN rotation lines. No gas was detected, with upper limits for CO ranging between $3.5\text{--}4.5 \times 10^{27}$ molec s^{-1} . Combined with published water production rate estimates we have generated ice sublimation models consistent with the photometric light curve. The inbound light curve is likely controlled by sublimation of CO₂. At these distances water is not a strong contributor to the outgassing. We also infer that there was a long slow outburst of activity beginning in late 2011 peaking in mid-2013 January ($r \sim 5$ AU) at which point the activity decreased again through 2013 June. We suggest that this outburst was driven by CO injecting large water ice grains into the coma. Observations as the comet came out of solar conjunction seem to confirm our models.

Subject headings: comets: general — comets: individual (ISON),

1. INTRODUCTION

On 2012 September 21 a new sungrazing comet was discovered using the 0.4-meter International Scientific Optical Network telescope in Russia (Nevski & Novichonok 2012). The comet was designated C/2012 S1 (ISON)

meech@ifa.hawaii.edu

¹ NASA Astrobiology Institute

² Institute for Astronomy, University of Hawaii, 2680 Woodlawn Drive, Honolulu, HI 96822, USA

³ European Southern Observatory

⁴ Max-Planck-Institut für Sonnensystemforschung, Max-Planck-Strasse 2, 37191, Katlenburg-Lindau, Germany

⁵ Queens Univ. Belfast, Belfast BT7 1NN, Northern Ireland

⁶ Dept. of Physics and Astronomy, University of Alaska Anchorage, 3211 Providence Dr., Anchorage, AK 99508

⁷ Gemini Observatory, Northern Operations Center, 670 N. Aohoku Place, Hilo, HI 96720, USA

⁸ Associazione Astronomica Euganea, via Tommaseo, 35131 Padova, Italy

⁹ BRIXIIS Observatory, Eyckensbeekstraat, 9150 Kruibeke, Belgium

¹⁰ Talmassons Observatory (C.A.S.T.), via Cadorna, 33030 Talmassons, Italy

¹¹ Stazione Astronomica Descartes, via Lambrinia 4, 2013 Chignolo Po', Italy

¹² INAF-Osservatorio Astrofisico di Arcetri, Largo E. Fermi 5, I-40125 Firenze, Italy

¹³ DLR-German Aerospace Center, Institute of Planetary Research, Rutherfordstr. 2, D-12489 Berlin, Germany

¹⁴ Indian Inst. Astrophys., II Block, Koramangala, Bangalor 560 034, India

¹⁵ JHU-APL, 11100 Johns Hopkins Road, Laurel MD 20723

^a Hubble Fellow

^b CARA Project, Astrofilii Italiani, IASF INAF via Fosso del Cavaliere 100, 00133 Roma, Italy

(hereafter comet ISON) and was bright and active at 6.3 AU pre-perihelion. The current estimate of its orbital eccentricity is 1.000004, thus it is possibly making its first passage through the inner solar system from the Oort cloud. Perihelion is on 2013 November 28 at a distance of 0.0125 AU (2.7 solar radii), and some predictions suggest it could become exceedingly bright. About a dozen comets in the past ~ 270 years have been spectacularly bright ($\text{mag} < -5$), and the hope that comet ISON could be one of these has generated intense scientific interest. However, it is difficult to predict the comet's behavior while still far from the Sun. Comet ISON was well placed for observation until moving into solar conjunction in 2013 June, and it emerged again in the dawn skies in late 2013 August, near $r=2.4$ AU. In this letter, we report observations of the comet at optical and submillimeter wavelengths from 2011 September through 2013 June. Based on these data and the gas production rates from the literature, we used an ice sublimation model to look at activity scenarios for when the comet emerged from solar conjunction.

2. OBSERVATIONS & DATA REDUCTION

We initiated both a pre-perihelion imaging campaign and a sub-mm observing campaign to constrain volatile production rates (see Table 1). Imaging data were taken on both photometric nights and nights with some cirrus. Calibrations on photometric nights were accomplished with measurements of Landolt (1992) standard stars. Fields on non-photometric nights and for Pan-STARRS1 (PS1) were calibrated against the Sloan Digital Sky Sur-

vey (SDSS; York *et al.* (2000)) or the PS1 2-pi survey (Magnier *et al.* 2013). Conversion to Kron-Cousins R-band used the transformation equations derived by R. Lupton¹⁸ and Tonry *et al.* (2012) assuming an observed color of $V - R = 0.4$ (Lisse *et al.* 2013).

2.1. Pan STARRS1

Comet ISON was detected in images obtained with PS1 and the Gigapixel Camera 1 (0.256'' pixels) between 2011 September and 2013 January during regular survey operations. Exposures were made in the survey *grizw_{P1}* filters. Moving objects are normally automatically detected and measured via difference imaging (Denneau *et al.* 2013). Before 2012 January the comet was moving too slowly and/or was too faint for this to be successful; these detections were made by manual inspection of the data post-discovery. In all PS1 prediscovery data the comet has a profile no wider than the point spread function (PSF) of field stars, although we infer it was likely to be active at this time (see §3.2). The magnitudes were measured via DAOPHOT PSF-photometry relative to field stars of known magnitudes (Schlafly *et al.* 2012). The 2012 January 28 detections were reported to the Minor Planet Center (MPC) within 24 hours. However as its motion was roughly parallel to the ecliptic, and the PSF was measured to be stellar, it was not reported as an object of interest. From 2012 September onwards the comet possessed a visible coma, and magnitudes were measured in the PS1 photometric system within a 5'' radius circular aperture (Schlafly *et al.* 2012; Magnier *et al.* 2013) when not contaminated by field stars.

2.2. UH2.2m, HCT2m, Lowell Observatory 1.8m, and Calar Alto 1.2m

We had several observing runs in 2012-2013 where we obtained data on comet ISON. The UH2.2m telescope on Mauna Kea was used with the Tek 2K CCD camera and Kron-Cousins filter. Data were obtained using the Himalayan Chandra telescope with the Optical 2K×4K imager (E2V chips with image scale of 0.17'' pix⁻¹) through Bessell R-band filters. Observations at the Lowell observatory were taken on the Perkins 1.8m telescope with the PRISM reimaging camera (SITE 2K×2K CCD) through the Bessell R band. Data were obtained under variable conditions during several nights using the Calar Alto 1.2m with the e2v CCD binned 2×2.

2.3. Gemini North 8-m

Director's discretionary time was awarded to image the comet monthly from 2013 February through June (see Fig. 1). Data were obtained using the GMOS-N multi-object spectrograph in imaging mode with the e2V CCD binned 2×2 resulting in a plate scale of 0.145'' pix⁻¹. Baseline calibrations were used in the reduction. Most of the images were obtained through the Sloan r'-filter (Fukugita *et al.* 1996). Some non-photometric nights were calibrated using the USNO-A2 catalog, resulting in a photometric accuracy of 5-10%.

2.4. JCMT

The radio observations were performed using the 15-m JCMT telescope on 15 days between 2013 March 9 through 2013 June 16. Long integration observations were performed on March 15 and 30, April 1, 27-29 and June 14-16. At other times, hourly snapshot observations were obtained. We used HARP and the R×A3 heterodyne receivers in beam-switch (*i.e.* secondary chopping) mode. The planets Mars and Uranus were frequently observed to monitor the main beam efficiency. The ACSIS spectrometer was used, which provides a total bandwidth of 250 MHz and a spectral channel spacing of 30.5 kHz. The data were reduced using a combination of the Starlink software and IDL scripts.

Searches for the J=3-2 and J=2-1 rotational transitions of CO gas and the J=4-3 and J=3-2 transitions of HCN gas returned negative results. HCN is an indicator of sublimated gas, but not expected to play a major role in controlling the brightness of the comet, so we focus only on the analysis of CO. To estimate production rates of CO, we measured the root-mean-square value of the main beam brightness temperature fluctuations within ±10 km s⁻¹ of zero velocity (see Table 1). Given that CO lines are likely to be narrow (Senay & Jewitt 1994; Biver *et al.* 2002), the 3-σ upper limits to the line area were derived within a 1.2 km s⁻¹ or 1.5 km s⁻¹ (for June only) band. We assume that gas molecules escape from the surface at a constant velocity and follow a Haser density distribution. We adopted an average expansion velocity of 1.12·r^{-0.41} km s⁻¹ and the kinetic temperature was estimated using an empirical formula of 116·r^{-1.24} K, where r is the heliocentric distance (Biver *et al.* 1997). The derived production rate upper limits, for the CO J(2-1) and J(3-2) transitions, are listed in Table 1.

2.5. The CARA Project

CARA is a consortium of amateur astronomers who have developed a standardized approach to observing comets. Photometry through a Cousins R-filter was obtained on 46 dates (Table 2) beginning shortly after discovery in 2012 September through 2013 May 2 with most of the observations coming from 0.4m telescopes at the BRIXIIS Observatory in Belgium, the Talmassons Observatory and Stazione Astronomica Descartes in Italy. The photometry was calibrated using the APASS catalog¹⁹.

2.6. VYSOS Telescope

We used the 5.3 inch Variable Young Stellar Objects Survey (VYSOS) program²⁰ robotic refractor at the Mauna Loa Observatory in Hawai'i, with an Apogee Alta U16M CCD (field of view 2.9×2.9 degrees with a plate scale of 2.53'' pixel⁻¹) to image the comet. Images were taken nearly nightly from 2013 April to mid-June (Table 2). On most nights, at least three exposures of 100 sec each were taken in a Sloan r'-band filter.

We used SExtractor²¹ to extract detections from our 165 VYSOS images, using an aperture that contained >95% of the PSF. We corrected for focal plane irregularities with an approximate distortion map, permitting us

¹⁸ <http://www.sdss.org/>

¹⁹ <http://www.aavso.org/apass>

²⁰ <http://www.ifa.hawaii.edu/~reipurth/VYSOS/>

²¹ <http://www.astromatic.net>

to match stellar detections between frames in the VYSOS run. We used the first image to perform relative photometric calibrations of subsequent images, and used overlapping stars from frame to frame for calibration—thus establishing a relative zero-point calibration spanning the entire run has a nominal uncertainty of 0.027 mag. For some VYSOS frames, the survey overlapped with SDSS, permitting us to calibrate one selected frame to 0.014 mag using 39 SDSS stars, establishing an absolute magnitude scale for the entire run. ISON’s ephemeris was used to search for it in the SExtractor catalogs and then measure it, finding an object within 4'' (<2 pixels) of its predicted location in 129 frames (the others were excluded because of chip gaps and field star proximity).

3. ANALYSIS & RESULTS

3.1. *Finson-Probstein Dust Modeling*

Finson-Probstein modeling (Finson & Probstein 1968) was used to analyze the synchro-syndyne pattern and the optical appearance of the comet’s dust environment (modeling details are described in Beisser (1987); Vincent (2010)). Due to projection, as seen from Earth the syndyne-synchro pattern converges in the direction of the dust tail, aligning with the central axis of the optical dust tail. The travel time of micron-sized dust through the dust tail in the images is ~ 20 -30 days. Larger grains of $\sim 100 \mu\text{m}$ size may stay much longer (~ 100 days) in the immediate (5'' radius) neighborhood of the nucleus. The width of the dust tail suggests a dust expansion speed of $\sim 10 \text{ m s}^{-1}$ assuming micron size dust grains dominate its optical appearance. It is reasonable to assume that larger ($100 \mu\text{m}$) grains leave the nucleus dust acceleration zone at a speed near one to a few m s^{-1} .

3.2. *Conceptual Ice Sublimation Model*

We used a simplified ice sublimation model to investigate the level of activity versus heliocentric distance. The model computes the amount of gas sublimating from an icy surface exposed to solar heating (Meech *et al.* 1986; Meech & Svoren 2004). As the ice sublimates, either from the nucleus surface or near-subsurface, the escaping gas entrains dust in the flow which escapes into the coma and tail. The scattered brightness of the comet as measured from Earth has a contribution from the light scattered from the nucleus and the dust. Model free parameters include the ice type, nucleus radius, albedo, emissivity, density, properties of the dust (sizes, density, phase function), and fractional active area.

Our model assumes a nucleus radius of $R_N \sim 2 \text{ km}$, consistent with the size limit inferred from Hubble Space Telescope (HST) measurements (Li *et al.* 2013), an albedo of 0.04 for both the nucleus and dust, and a linear phase function of $0.04 \text{ mag deg}^{-1}$ typical of other comets. We assume a nucleus density of 400 kg m^{-3} similar to that seen for comets 9P/Tempel 1 and 103P/Hartley 2 (Thomas *et al.* 2013a,b), a grain density of 1000 kg m^{-3} , and micron-sized grains (see §3.1 and Yang (2013)). Because of the many model free parameters, our conclusions are dependent on how well we can constrain some of the values with observations. The shape of the light curve—*i.e.* where the curve is steep or shallow—is determined by the sublimating ice composition. With reasonable estimates of nucleus size, albedo, density, and grain

properties, the fractional active surface area is adjusted to produce the observed volatile production rates. Note, if the HST nucleus size is much smaller than the upper limit used here, the model will require an increase in the active fractional area, but otherwise the discussion below remains unchanged.

Because the comet was active at discovery ($r=6.3 \text{ AU}$) where it was too cold for significant water-ice sublimation, there must be another volatile besides H_2O responsible for the outgassing. The likely candidates are CO and CO_2 . The warm *Spitzer* measurements on June 13 (Lisse *et al.* 2013) detected an excess brightness at $4.5 \mu\text{m}$ due to emission from a neutral gas coma which could either be due to CO_2 or CO (because both have lines in the bandpass). Unfortunately, there have been no definitive spectral detections of either molecule reported yet, however the similarity of the estimated CO_2 production rate to measurements of other comets at large distances (Ootsubo *et al.* 2012) suggested that CO_2 dominated. We ran two models, assuming the excess seen by *Spitzer* was either all CO or CO_2 (see Table 3) and the best fit models are shown in Fig. 2a. While both models can fit the inferred *Spitzer* and water production rates, and match the scattered light data from the dust in 2013 June, neither model alone is a good match to the light curve.

Our June CO production upper limits (which agreed with preliminary estimates from HST, M. A’Hearn, private comm., 2013), also suggested that the *Spitzer* observations were mostly CO_2 . With this scenario, however, the only explanation for the light curve between 6-3.5 AU was a long slow outburst, driven most likely by CO (and supported by a possible CO detection, N. Biver, private communication, 2013). Such a scenario is physically plausible, as evidenced by the aperiodic CO driven outbursts of Comet 29P/Schwassmann Wachmann 1 at similar distances (Cochran *et al.* 1982; Crovisier *et al.* 1995).

While we were preparing the models, an amateur astronomer, B. Gary²² reported the recovery of the comet as it came out of solar conjunction on 2013 August 12 and 16 at 7 airmasses. These magnitudes are also included in Table 1. At $r=2.5 \text{ AU}$, H_2O sublimation should be important and we added this to the model and found that with a fractional active area of 2.5% for water sublimation and 0.54% for CO_2 , the model fit both the 2013 August data and the early PS1 data with the comet being largely controlled by CO_2 outgassing as shown in Fig. 2b.

If we allow that solar heat from the inbound orbit reached a deeper layer of CO this could trigger additional outgassing starting around the time of the first PS1 observations. The effect was a period of increased activity reaching a maximum effective sublimating area of $\sim 3.4\%$ at $r=5.1 \text{ AU}$ in 2013 January, and linearly dropping off and ceasing activity in mid July. This increase is shown as the dotted line in Fig. 2b. The difference between the observations and the CO_2 plus H_2O model is shown in Fig. 2c which represents the CO outburst. The predicted CO production rates during this time are shown in Table 3.

Matching water production estimates from 2013 March 5 and May 4 (Schleicher (2013a,b); see Table 3), re-

²² brucegary.net/ISON

quired that the effective water-ice sublimating area was $\sim 6\times$ that of the nucleus surface in March dropping to $\sim 80\%$ of the surface in May as the heliocentric distance decreased. The model run-out was also consistent with all of the other H_2O production rate upper limits shown in Table 3. As was seen for 103P/Hartley 2 (A’Hearn *et al.* 2011), we propose that this outburst ejected large water ice grains into the coma. It has been shown experimentally that sublimation from deeper layers can result in the ejection of large slow-moving grains (Laufer *et al.* 2005). A long-lived population of large ($\sim 100\mu\text{m}$) water-ice grains in the near nucleus environment could explain this water production behavior.

Dirty (low albedo) ice grains of this size could survive for months at the low temperatures outside $r=8$ AU, however inside 6 AU they would not survive very long (Hanner 1981). On the other hand, for moderately high albedo grains ($p_v > 0.5$) lifetimes of months to days are possible from $r=6$ to 3.5 AU (2012 September through 2013 May). As noted in § 3.1, grains this large would not contribute optically to the tail structure as they would remain close to the nucleus in projection. Once in the coma, the water ice grains slowly sublimate, releasing dust into the coma and increasing its cross section. With high albedos and long grain lifetimes, the duration of the brightening by this mechanism could be many months (e.g. 2012 January-2013 January). The fading was not caused by loss of large grains from the aperture, grains that would survive for the duration are so large that they stay within the $5''$ radius aperture (equivalent to $\sim 15,000$ km) in 2013 January. At a typical velocity of 1 m s^{-1} the crossing time for the aperture is \sim months. The effective brightness decline (compared to an expected increase from sublimation as r decreased) was thus a loss of cross section within the aperture. With the limited data we have, we cannot say if the outburst was short-lived, or if there was continued activity, although possible detections of CO after 2013 January suggest that there was outgassing for a period of time.

4. DISCUSSION

In formulating the concept of the Oort cloud (Oort & Schmidt 1951), Oort suggested that the dearth of returning long-period comets at large semi-major axis was due to chemical alteration of their surface layers by cosmic rays, and that this ‘volatile frosting’ was lost on the first passage through the inner solar system. One interpretation of comet ISON’s heliocentric light curve could be its activity through 2013 January was dominated by the loss of this highly volatile layer, and the activity since then has been decreasing. The implication of this interpretation is that the comet will not brighten as dramatically as hoped near perihelion, and that the apparent brightness coming out of solar conjunction would have remained flat or even decreased. This is similar to the behavior observed for Comet C/1973 E1 (Kohoutek).

In the second scenario for activity where the comet is largely driven by CO_2 outgassing, our models predicted that the apparent brightness within a $5''$ radius aperture should be $\sim R=14-14.5$ when the comet came out of solar conjunction in late August/early September matching closely what has occurred. While it is unwise to make predictions about the brightness at perihelion when the comet is still far from the sun, especially when it will

pass so close to the sun, the run out of these sublimation models show that the comet can still be quite bright at perihelion.

Gemini is operated by AURA under a cooperative agreement with the NSF on behalf of the Gemini partnership. The James Clerk Maxwell Telescope is operated by the Joint Astronomy Centre on behalf of the Science and Technology Facilities Council of the United Kingdom, and the National Research Council of Canada. Data were acquired using the PS1 System operated by the PS1 Science Consortium (PS1SC) and its member institutions. The Pan-STARRS1 Surveys (PS1) have been made possible by contributions from PS1SC member Institutions and NASA through Grant NNX08AR22G, the NSF under Grant No. AST-123886, the Univ. of MD, and Eotvos Lorand Univ.. B.Y., T.R. and K.J.M. acknowledge support through the NASA Astrobiology Institute under Cooperative Agreement NNA08DA77A. H.H.H. is supported by NASA through Hubble Fellowship grant HF-51274.01 awarded by the Space Telescope Science Institute, which is operated by the Association of Universities for Research in Astronomy for NASA, under contract NAS 5-26555. We also thank the following CARA observers for their contributions: Giovanni Sostero, Ernesto Guido, Nick Howes, Martino Nicolini, Herman Mikuz, Daniele Carosati, Jean Francois Soulier, Man-To Hui, Gianni Galli, Walter Borghini, Paolo Bacci and Diego Tirelli.



FIG. 1.— Images of comet ISON obtained using the Gemini 8m with GMOS on 2013 February 4, March 4, April 3, May 4 and 30 through an r filter. The May 4 image is a color composite image made using the g , r and i images. East is left, N is up and the FOV is $\sim 2.5'$ wide per panel (corresponding to a projected distance of $4.25\text{--}4.70 \times 10^5$ km at the distance of the comet).

REFERENCES

- A'Hearn, M.F., Belton, M.J.S., Delamere, W.A. *et al.* 2011, *Science*, 332, 1396
 Beisser K., 1987, diploma thesis, University Erlangen
 Biver, N., Bockelée-Morvan, D., Colom, P. *et al.* 1997, *EM&P*, 78, 5
 Biver, N., Bockelée-Morvan, D., Colom, P. *et al.* 2002, *EM&P*, 90, 5
 Bodewits, D., Farnham, T., A'Hearn, M.F. 2013, *CBET* 3608.
 Cochran, A.L., Cochran, W.D., Barker, E.D. 1982, *ApJ*, 254, 816
 Crovisier, J., Biver, N., Bockelée-Moran, D. *et al.* 1995, *Icarus*, 115, 213
 Denneau, L., Jedicke, R., Grav, T. *et al.* 2013, *PASP*, 125, 357
 Finson, M.L., Probst, E.F. 1968, *ApJ*, 154, 353
 Fukugita, M., Ichikawa, T., Gunn, J.E., *et al.* 1996, *AJ*, 111, 1748
 Hanner, M.S. 1981, *Icarus*, 47, 342
 Landolt, A. 1992, *AJ*, 104, 340
 Laufer, D., Pat-El, I., Bar-Nun, A. 2005, *Icarus*, 178, 248
 Li, J.-Y., Weaver, H.A., Kelley, M.S., *et al.* 2013, *CBET* 3496
 Lisse, C.M., Vervack, R.J., Weaver, H.A. *et al.* 2013, *CBET* 3598
 Magnier, E.A., Schlafly, E., Finkbeiner, D., 2013, *ApJS*, 204, 20
 Meech, K.J., Jewitt, D., & Ricker, G.R. 1986, *Icarus*, 66, 561
 Meech, K.J. & Svoren, J. 2004, in *Comets II*, ed. M.C. Festou *et al.* (Univ. AZ Press), 317-335
 Nevski, B., Novichonok, A. 2012, *CBET* 3238
 Oort, J.H., Schmidt, M. 1951, *BAN* 11, 259
 Ootsubo, T., Kawakita, H., Hamada, S. *et al.* 2012, *ApJ*, 752, 15
 Schlafly, E.F., Finkbeiner, D.P., Jurić, M. *et al.* 2012, *ApJ*, 756, 158
 Schleicher, D.G 2013a, *IAUC* 9254.
 Schleicher, D.G 2013b, *IAUC* 9257.
 Senay, M. C., & Jewitt, D. 1994, *Nature*, 371, 229
 Thomas, P.C., A'Hearn, M., Belton, M.J.S., *et al.* 2013a, *Icarus* 222, 453
 Thomas, P.C., A'Hearn, M.F., Veverka, J. *et al.* 2013b, *Icarus* 222, 550
 Tonry, J.L., Stubbs, C.W., Lykke, K.R., *et al.* 2012, *ApJ*, 750, 99
 Vincent J.-B., 2010, PhD thesis, Technical University Braunschweig
 Yang, B. 2013, *CBET* 3622.
 York, D.G. *et al.* 2000, *AJ*, 120, 1579

TABLE 1
OBSERVATIONS

UT Date	Telescope	N ^a	t ^b	Filter	r^c	Δ^d	α^e	TA ^f	PA _{-\odot} ^g	PA _{-v} ^h	m_R^i
2011-09-30	PS1	4	180	w_{P1}	9.392	9.679	5.77	-175.83	284.9	299.8	20.91±0.12
2011-11-10	PS1	2	90	i_{P1}	9.064	8.669	5.87	-175.75	278.4	294.5	20.64±0.11
2011-11-26	PS1	2	86	g_{P1}	8.934	8.302	5.05	-175.72	274.2	293.4	20.42±0.10
2011-12-09	PS1	2	30	z_{P1}	8.829	8.043	4.04	-175.69	268.9	293.2	19.92±0.12
2012-01-05	PS1	1	43	g_{P1}	8.606	7.643	1.41	-175.63	226.3	302.9	19.55±0.09
2012-01-28	PS1	2	90	w_{P1}	8.416	7.491	2.44	-175.58	125.4	61.9	19.67±0.02
2012-10-11	HCT2m	5	1500	R	6.089	6.212	9.26	-174.80	284.9	297.2	17.49±0.01
2012-10-14	Calar Alto 1.2m	7	1800	R	6.067	6.155	9.32	-174.79	284.7	297.0	17.49±0.02
2012-11-08	UH2.2m	2	600	R	5.814	5.474	9.46	-174.68	281.1	294.0	17.12±0.01
2012-11-22	Lowell 1.8m	3	1800	VR	5.672	5.114	8.68	-174.70	278.0	292.5	16.87±0.01
2012-12-20	Lowell 1.8m	3	1800	R	5.383	4.502	5.10	-174.47	264.3	290.3	16.32±0.01
2012-12-23	PS1	4	180	w_{P1}	5.350	4.446	4.55	-174.46	261.1	290.4	16.35±0.03
2013-01-03	PS1	1	40	r_{P1}	5.234	4.275	2.62	-174.40	238.3	292.8	16.02±0.04
2013-01-06	Calar Alto 1.2m	3	900	R	5.199	4.231	2.15	-174.37	223.3	295.5	16.08±0.03
2013-01-13	Lowell 1.8m	2	1200	R	5.129	4.157	1.87	-174.34	177.9	313.7	16.81±0.01
2013-02-04	Gemini N 8m	2	150	r	4.891	4.019	5.95	-174.20	113.2	85.6	15.88±0.10
2013-03-04	Gemini N 8m	2	90	r	4.578	4.050	11.19	-174.01	99.1	84.4	15.90±0.10
2013-04-03	Gemini N 8m	4	197	r	4.231	4.206	13.61	-173.77	93.0	80.3	15.87±0.10
2013-05-01	Calar Alto 1.2m	4	1200	R	3.886	4.326	12.70	-173.50	90.2	75.6	15.92±0.02
2013-05-04	Gemini N 8m	3	135	gr_i	3.857	4.331	12.50	-173.48	90.0	75.1	15.61±0.10
2013-05-17	UH2.2m	4	1200	R	3.693	4.341	11.13	-173.42	89.6	73.6	15.85±0.01
2013-05-30	Gemini N 8m	2	90	r	3.528	4.318	9.34	-173.18	87.6	66.2	15.65±0.01
2013-08-12	G95 ^j 11-in			R	2.487	3.418	7.88	-171.89	294.2	311.3	14.73±0.10
2013-08-16	G95			R	2.425	3.332	9.07	-171.79	293.1	309.1	14.71±0.10
UT Date	Telescope	Mol.	Line	f^k	t_{int}^l	B_{eff}^m	r	Δ	rms ⁿ	TP	QCO^q
2013-03-10,15	JCMT	CO	J(3-2)	345.8	7500	0.52	4.47	4.09	6.1	18	<3.9
2013-03-30	JCMT	CO	J(3-2)	345.8	6468	0.50	4.26	4.19	5.5	19	<3.5
2013-04-01	JCMT	CO	J(3-2)	345.8	6468	0.50	4.26	4.19	5.5	19	<3.5
2013-04-27,28	JCMT	CO	J(2-1)	230.5	9156	0.50	3.93	4.32	4.6	21	<4.5
2013-06-14,15	JCMT	CO	J(2-1)	230.5	15042	0.50	3.32	4.23	3.2	26	<4.1

^a Number of exposures.

^b Total integration time, s.

^c Heliocentric distance, AU.

^d Geocentric distance, AU.

^e Solar phase angle, degrees.

^f True anomaly, degrees.

^g Position angle of the antisolar vector, degrees East of North.

^h Position angle of the negative velocity vector, degrees East of North.

ⁱ Mean apparent R-band magnitude.

^j Hereford Arizona Observatory

^k Rest Frequency, in GHz.

^l Total integration time, s.

^m Main Beam Efficiency.

ⁿ 1- σ rms noise in unit of the main beam brightness temperature, in mK.

^p Kinetic temperature computed based on the formula from Biver *et al.* (1997), in K.

^q 3- σ production rates upper limits for CO, in 10²⁷ molec s⁻¹.

TABLE 2
CARA AND VYSOS OBSERVATIONS

UT Date	Tel. ^a	N	t	Filter	r	Δ	α	TA	PA _{-\odot}	PA _{-v}	m_R
2012-09-25	CARA-Net			R	6.250	6.636	8.240	-174.868	286.8	299.7	17.69±0.21
2012-10-04	CARA-Net			R	6.161	6.405	8.850	-174.831	285.8	298.3	17.05±0.10
2012-10-10	CARA-Net			R	6.103	6.251	9.167	-174.807	285.1	297.4	17.10±0.20
2012-10-22	CARA-Net			R	5.985	5.931	9.566	-174.756	283.6	295.9	17.01±0.17
2012-10-23	CARA-Net			R	5.978	5.912	9.579	-174.753	283.5	295.8	17.07±0.20
2013-04-02	VYSOS	3	300	r	4.242	4.201	13.589	-173.78	93.2	80.4	16.10±0.06
2013-04-03	VYSOS	6	600	r	4.232	4.205	13.608	-173.77	93.0	80.3	15.68±0.02
2013-04-04	VYSOS	3	300	r	4.220	4.211	13.627	-173.76	92.9	80.1	15.89±0.04
2013-04-05	VYSOS	3	300	r	4.208	4.216	13.642	-173.75	92.8	80.0	15.90±0.04
2013-04-06	VYSOS	3	300	r	4.196	4.222	13.653	-173.75	92.7	79.9	15.89±0.05

^a See notes for Table 1

^b Table 2 is published in its entirety in the electronic edition. A portion is shown here for guidance regarding its form and content.

TABLE 3
2013 VOLATILE FLUX CONSTRAINTS

UT Date 2013	JD ^a	r^b	TA ^c	Q_{CO}^d	$Q_{CO_2}^d$	$Q_{H_2O}^d$	Facility	Ref ^e	Model Q_{CO}^f
January 30	56323	4.94	-174.23			<1E28	Swift	1	
March 5	56356	4.57	-174.00			3E26	Lowell	2	
March 11	56363	4.50	-173.96			<1E28	Swift	1	
March 10-15	56365	4.52	-173.97	<3.9E27			JCMT	3	1.9E27
March 30-April 1	56382	4.28	-173.80	<3.5E27			JCMT	3	1.7E27
April 24	56407	3.98	-173.58			<1E28	Swift	1	
April 27-28	56410	3.95	-173.55	<4.5E27			JCMT	3	1.5E27
May 4	56417	3.86	-173.48			6E26	Lowell	5	
May 9	56422	3.79	-173.42			<1E28	Swift	1	
June 13	56457	3.34	-173.00	2.1E27	1.9E26		Spitzer	6	7.0E26
June 14-15	56458	3.33	-172.98	<4.1E27			JCMT	3	7.0E26

^a Julian date-2400000.

^b Heliocentric distance, AU.

^c True anomaly, degrees.

^d Production rate, molec s⁻¹.

^e References: 1-(Bodewits *et al.* 2013), 2-(Schleicher 2013a), 3-this paper, 4-A'Hearn private comm, 5-(Schleicher 2013b), 6-(Lisse *et al.* 2013).

^f CO production rate prediction from model CO outburst.

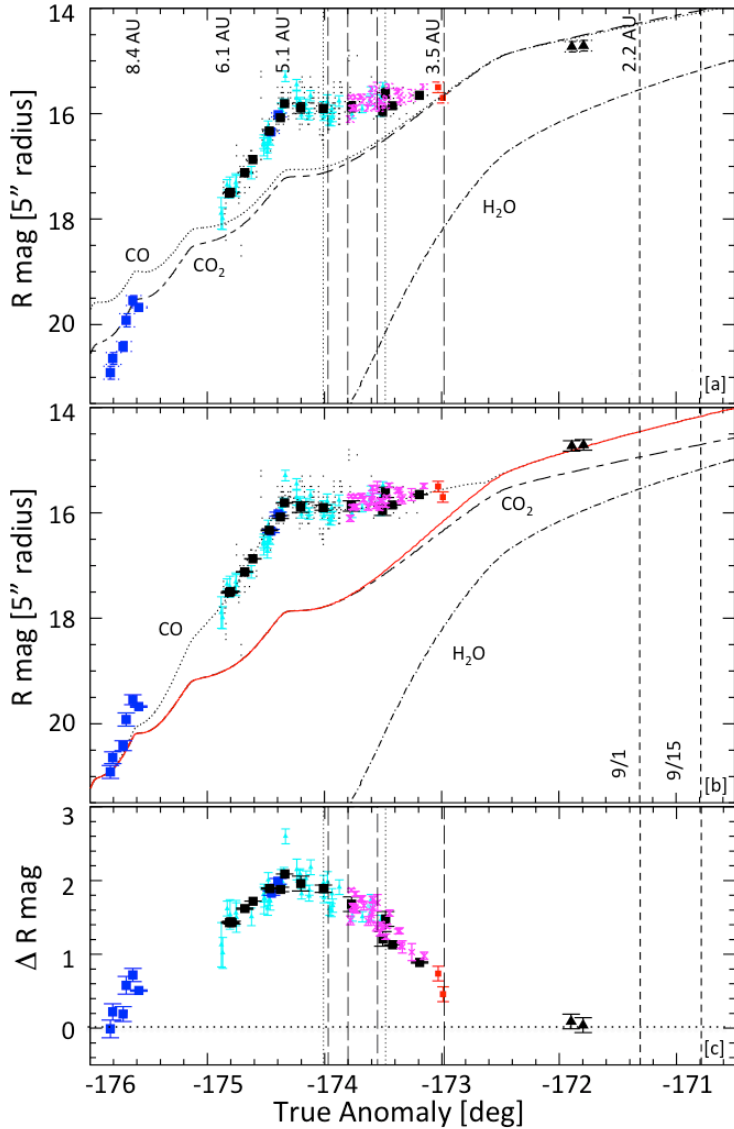


FIG. 2.— Conceptual ice sublimation model, showing the best fit for 2013 June 13 (TA=-173.0). The different ice models are for H₂O (dot-dash), CO₂ (long-short dash), CO (dotted) and total (solid red line). The large telescope photometric measurements are shown as large black squares, the PS1 pre-covery data as blue squares, the CARA data as cyan triangles, the data from VYSOS as the magenta crosses, and data as reported in the MPECs as black dots (uncorrected for aperture size). The optical data obtained at the time of the *Spitzer* observations (Lisse *et al.* 2013) are shown as small red squares. The reported measurements by B. Gary are shown as black triangles. The vertical dotted lines show the dates for which Q_{H_2O} has been published. The vertical long dashed lines show the dates where we present JCMT Q_{CO} upper limits and the short dashed lines indicate when the comet will likely become accessible to large telescopes as it comes out of solar conjunction. [a] Best fit models assuming that all the reported *Spitzer* outgassing is due to only CO or CO₂. [b] Best fit model with baseline CO₂ plus H₂O sublimation with an additional slow CO outburst. [c] Difference between the data and sublimation model, showing the outburst.